

Heat Transfer Analysis of Ground-Coupled Structures

E.A. Rodriguez

S. Alvarez, Ph.D.

ABSTRACT

In this paper, a transient two-dimensional method for analyzing heat transfer through ground-coupled elements in a building is described. The heat conduction differential equation is solved by using a numerical scheme based on the eigenvalue technique. The solution is carried out by means of the superposition principle and incorporates a harmonic representation of the outside climatic conditions. A set of examples is given in graphical outputs to show some aspects of the modeling.

INTRODUCTION

The stability of the earth temperature with respect to diurnal cycles and extreme meteorological conditions makes the ground a useful heat source in winter and heat sink in summer.

From an energy conservation viewpoint, earth-sheltered buildings, underground or earth-covered, can provide (in most climatic regions) excellent heating and cooling potential.

Until recently, heat transfer analyses related to underground surfaces were based on one-dimensional steady-state assumptions. This fact leads to errors when dealing with partially insulated structures (Wang 1981) and, in any case, these methods are only valid for estimating winter design loads in cold climates.

In recent years, finite-difference and finite-element numerical techniques have been successfully applied to a variety of earth-coupled building heat transfer problems (see, for instance, Ceylan and Myers 1979; Shipp et al. 1981; Mitalas 1983; and Mokhtari et al. 1987). However, most of them have been oriented to parametric studies on insulation configurations, etc.

As a consequence, these methods are not well-suited to be coupled to the internal excitations that may appear in earth-sheltered buildings.

STATEMENT OF THE PROBLEM

Figure 1 shows a cross section of one of the systems capable of being analyzed. In order to consider the different behavior of the interior surfaces of the building, we have identified four different zones: basement wall below grade with insulation (zone 1), basement wall below grade without insulation (zone 2), basement floor adjacent to the wall (zone 3), and the remainder of the basement floor (zone 4).

Assuming bidimensional conduction and constant properties, the governing heat transfer partial differential equation is:

E.A. Rodriguez, Mechanical Engineer, and S. Alvarez, Professor of Thermal Energy, Engineering School, University of Seville, Spain.

$$\frac{\partial^2 T}{\partial x^2} + \frac{\partial^2 T}{\partial y^2} = \frac{1}{\alpha} \frac{\partial T}{\partial t} \quad (1)$$

where

$$\begin{aligned} T &= \text{temperature of the medium } (^{\circ}\text{C}) \\ \alpha &= \text{thermal diffusivity } (\text{m}^2/\text{s}) \\ t &= \text{time (s)} \end{aligned}$$

The boundary condition at the ground surface is expressed by an energy balance which includes the conduction heat flow into the ground, the convective heat transfer between the surface and the ambient air, the absorbed solar radiation, the long-wave radiant exchange with the surroundings, and the latent heat of evaporation. This energy balance may be put in a very convenient form by making use of the sol-air temperature concept (T_{sa}) (ASHRAE 1985) as:

$$-\lambda \frac{\partial T}{\partial x} = h(T_{sa} - T) \quad (2)$$

where

$$\begin{aligned} \lambda &= \text{thermal conductivity } (\text{W/m}^{\circ}\text{C}) \\ h &= \text{convective-radiant heat transfer coefficient at the surface } (\text{W/m}^2 \text{ } ^{\circ}\text{C}) \end{aligned}$$

The periodic nature of the external excitations suggests a harmonic formulation to represent the evolution of T_{sa} . According to Molina (1987), it is approximate enough to consider three frequencies of 1 (annual), 365 (daily), and 730 cycles per year. Consequently, we can write:

$$T_{sa} = \bar{T}_{sa} + \sum_{i=1}^3 A_i \cos(\omega_i t + \phi_i) \quad (3)$$

where

$$\begin{aligned} \bar{T}_{sa} &= \text{annual mean value of } T_{sa} \\ A_i &= \text{amplitude of i-th harmonic} \\ \omega_i &= \text{frequency of i-th harmonic} \\ \phi_i &= \text{phase-shift of i-th harmonic} \end{aligned}$$

In fact, considering the filter effect caused by the very high thermal capacity of the ground, only the first harmonic (corresponding to the annual cycle) would be significant in the responses of most zones.

The isothermal boundary condition is the temperature of the groundwater table (if existing) or the natural deep ground temperature. In order to simplify the calculations, it has been supposed to be equal to the annual mean value of T_{sa} .

Finally, the boundary conditions at the internal surfaces of the four zones identified have been taken as prescribed temperatures. These temperatures are the coupling variables with the internal excitations and cannot be calculated independently of them.

MODEL DESCRIPTION

For solving the problem, a finite-difference method has been used. With only a spatial discretization both Equation 1 and the boundary conditions are replaced by a system of first-order ordinary differential equations, which can be represented in matrix notation as:

$$[C] \cdot [\dot{T}] = [K] \cdot [T] + [B] \cdot [U] \quad (4)$$

where $[C]$ is the capacitance matrix whose values are the thermal capacitances per unit width associated with each node of the model; $[K]$ is the conductance matrix which contains the thermal conductances between the discrete regions; and $[B] \cdot [U]$ is the input vector obtained from the external and internal excitations (boundary conditions).

First we have to solve the homogeneous problem:

$$[C] \cdot [\dot{T}] = [K] \cdot [T] \quad (5)$$

from which we obtain the diagonal eigenvalue matrix $[L]$ and the eigenvector matrix $[P]$.

In order to handle the time dependence of the input vector, we use the Duhamel's theorem and, defining a new vector $[X]$ as $[T] = [P] \cdot [X]$, the exact solution of Equation 4 can be written as:

$$[X(t)] = \exp([L]t) \left([X(0)] + \int_0^t \exp(-[L]\tau) \cdot [P]^t \cdot [B] \cdot [U(\tau)] d\tau \right) \quad (6)$$

where $[P]^t$ is the transpose of $[P]$.

The steady-state solution is given by this expression:

$$[X] = -[L]^{-1} \cdot [P]^t \cdot [B] \cdot [U] \quad (7)$$

Once the temperature distribution has been found, the heat flows at the boundaries can be readily computed from the discrete expression of the Fourier law by using the temperatures at the boundary and at nodal points of the vicinity. These expressions can be put in matrix form as follows:

$$[Q] = [S] \cdot [T] + [E] \cdot [U] = [S] \cdot [P] \cdot [X] + [E] \cdot [U] \quad (8)$$

The heat transfer at walls and floors in contact with the ground involves terms of very different time constants, ranging from the order of the hour for internal excitations to the order of a month for outside excitations.

The linear nature of the equations allows us to apply the superposition principle and to split the whole problem into three simpler ones (Figure 2).

Problem I

Calculation of the steady-state heat flow at the interior surfaces with the following boundary conditions:

Sol-air temperature	$T_{sa} = \bar{T}_{sa}$
Deep ground temperature	$T_g = \bar{T}_{sa}$
Interior surface temperatures	$T_i = 0$

The resulting heat flow component for each zone, i , can be expressed as:

$$q_i^I = S_{o,i} \bar{T}_{sa} + S_{g,i} \bar{T}_{sa} \quad (9)$$

where

S_o = conduction shape factor between the interior surface and the outside

S_g = conduction shape factor between the interior surface and the deep ground

Both S_o and S_g are obtained from the steady-state solution of Equation 8.

Problem II

Calculation of the harmonic heat flow at the interior surfaces of the building according to these boundary conditions:

Sol-air temperature	$T_{sa} = A \cos(\omega t + \phi)$
Deep ground temperature	$T_g = 0$
Interior surface temperatures	$T_i = 0$

The expression for the heat flow is:

$$q_i^{II} = S_{o,i} \sigma_i A \cos(\omega t + \phi + \Theta_i) \quad (10)$$

where

$$\begin{aligned}\sigma_i &= \text{amplitude decrement factor} \\ \Theta_i &= \text{phase-shift}\end{aligned}$$

Problem III

Calculation of the transient heat flow at the interior surfaces when the only excitations are the surface temperatures T_i and accordingly, $T_{sa} = T_g = 0$. In this case, it may be proved that a one-dimensional approach to each zone does not yield significant errors. The Z-transfer function technique (Stephenson and Mitalas 1971) can then be applied and the resulting heat flow is written as:

$$q_i^{III} = - \sum_{n=0}^{nc} C_{n,i} T_i(t - n\Delta t) + \sum_{n=1}^{nd} D_{n,i} q_i^{II}(t - n\Delta t) \quad (11)$$

where C_n and D_n are the coefficients of the Z-transfer function.

To calculate these coefficients, each zone is assumed to be a one-dimensional wall that incorporates an additional ground layer of around 50 cm. This thickness is a compromise obtained from inspection of a large set of cases. The calculation procedure could also be the eigenvalue technique previously described applied to a multilayered wall, or more standard methods (Stephenson and Mitalas 1971).

After calculating these Z-transfer function coefficients, they have to be corrected so as to fulfill the steady-state balance based on the simultaneous use of one-dimensional and two-dimensional approaches.

This steady-state balance leads to the equation:

$$\frac{- \sum_{n=0}^{nc} C_{n,i}}{1 + \sum_{n=1}^{nd} D_{n,i}} = S_{o,i} + S_{g,i} \quad (12)$$

The methodology followed to correct these coefficients is based in modifying only the last C_i coefficients by multiplying them by a common constant μ :

$$\begin{aligned}C'_n &= C_n \quad n = 0, \dots, nc/2 \\ C'_n &= \mu C_n \quad n = nc/2 + 1, \dots, nc\end{aligned}$$

The reason is that the first C_i coefficients reflect very well the responses caused by the actual and closest previous steps of calculation, so they should not be modified.

The constant μ is given by the following expression:

$$\mu = \frac{(1 + \sum_{n=1}^{nd} D_n)(U - S)}{\sum_{n=nc/2}^{nc} C_n} \quad (13)$$

where

$$S = S_o + S_g$$

U = global heat transfer coefficient of the wall + 50 cm of soil

Equations 9, 10, and 11 (this last containing the corrected C'_i coefficients) are now added to obtain the overall heat flow at zone i . The resulting equation can be written as:

$$q_i(t) = q_i^I + q_i^{II} + q_i^{III} = G_i(t) + C'_{0,i} T_i(t) \quad (14)$$

where $G_i(t)$ is a coefficient that contains information about present T_{sa} and T_g values and about the past history of inputs and heat flows.

COMMENTS ABOUT THE HYPOTHESES

Recalling the main hypotheses retained in the formulation of Equation 14, we have assumed:

1. Only one harmonic to represent the external excitations.
2. Uniform temperatures in each zone.
3. One-dimensional calculation of Z-transfer function coefficients.

The first two hypotheses are not inherent to the methodology.

Hypothesis 1 might be removed by retaining as many harmonics as necessary for a certain level of accuracy in the representation of T_{sa} .

Hypothesis 2 introduces a simplification in the same way as it is considered in conventional flat elements (walls) of a building. Anyway, in order to reduce the influence of this assumption, it can be selected as many different zones as expected to have nearly uniform temperature.

Hypothesis 3, however, has a two-fold effect on the results:

- The Z-transfer coefficients do not satisfy the steady-state balance and must be corrected in a proper way (already done above).
- Cross-influence between zones is neglected (see below).

If two adjacent zones in the ground structure exist with different thermal resistances (for instance, Zones 1 and 2 in Figure 1), the assumption of one-dimensional Z-transfer coefficients makes us overestimate the heat flow through one of the zones (the zone with the lowest thermal resistance) and underestimate the one through the other zone (the zone with the highest thermal resistance).

The reason for this fact is that we are neglecting the effect of the temperature of each zone in the heat flow of the other.

Figures 3 and 4 show the evolution in a one-year time period of the heat flows through Zones 1 and 2, respectively, corresponding to a structure similar to that in Figure 1. The composition of the vertical wall is given in the table below (in SI units).

ZONE	LAYER	THICKNESS m	CONDUCTIVITY $W/m^o C$	DENSITY kg/m^3	HEAT CAPACITY $J/kg^o C$
1	Concrete	0.20	0.50	1540	1100
	Aislant	0.05	0.03	40	1590
2	Concrete	0.25	0.50	1540	1100

The external excitation is:

$$\left. \begin{array}{l} \overline{T_{sa}} = 23^oC \\ A = 13^oC \\ \phi = 3.19rad \end{array} \right\} T_{sa}(t) = \overline{T_{sa}} + A \cos(\omega t + \phi)$$

The indoor air temperature is always kept at 20^oC , T_g is 23^oC , and the combined convective-radiant heat transfer coefficient is $9W/m^2 oC$.

In the mentioned figures, solid lines correspond to the responses given directly by the bidimensional model, while dashed lines are the heat flows given by the superposition method with the one-dimensional assumption for the Z-transfer coefficient calculation. Errors of around 21% and 18% are detected at the peak flows of Zones 1 and 2, respectively.

There is a simple way to damp down these errors without removing that convenient one-dimensional hypothesis. First of all, the conduction shape factors of the steady-state case (Problem I) must be calculated assuming fixed interior air temperature instead of surface temperatures (a typical value of the interior heat transfer coefficient must be chosen). This is a more realistic situation that lets the different zones reach their own spontaneous temperature.

Secondly, those air-to-air factors must be converted to air-to-surface factors by this expression:

$$S_i = \frac{1}{\frac{1}{S'_i} - \frac{1}{h_i}}$$

where

- S'_i = air-to-air conduction shape factor
- S_i = air-to-surface conduction shape factor
- h_i = interior combined heat transfer coefficient

This conversion lets us consider variable interior film coefficients when coupling with indoor conditions. After using this methodology, we reach better agreement in the results of the same example described above. Figures 5 and 6 show these results for each zone, presenting a maximum error of 3% in the Zone 2

CONCLUSIONS

The formulation developed to solve the heat transfer analysis of ground-coupled structures provides a practical way to handle the different time scales that appear together in these large inertia thermal problems.

Moreover, the closed form of Equation 14 allows the use of T_i as coupling variables with other heat transfer mechanisms involved (convection and radiation) and so is a good choice for building energy simulation codes.

REFERENCES

- ASHRAE.** 1985. handbook of Fundamentals, p. 26.4. Atlanta: American Society of Heating, Refrigerating, and Air-Conditioning Engineers, Inc.
- Ceylan, H.T., and Myers, G.E.** 1979. "Long-time solutions to heat-conduction transients with time-dependent inputs". A.S.M.E. Journal of Heat Transfer, Vol. 102, pp. 111-116.
- Mitalas, G.P.** 1983. "Calculation of basement heat loss". ASHRAE Transactions, Vol. 89, pp. 420-437.
- Mokhtari, M.; Roux, J.J., and Achard, G.** 1987. "Analyse modale et simulation thermique des locaux en contact avec le sol". Proceedings of the JITH'87, Renewable Energies and Rational Energy Utilisation. Lyon, pp. 566-573.
- Molina, J.L.** 1987. "Simulación energética de edificios mediante un modelo de respuesta en frecuencia". Doctoral dissertation thesis, Engineering School, University of Seville.
- Shipp, P.H.; Pfender, E., and Bligh, T.P.** 1981. "Thermal characteristics of a large earth-sheltered building, parts I and II". Underground Space, Vol. 6, pp. 53-64.
- Stephenson, D.G., and Mitalas, G.P.** 1971. "Calculation of heat conduction transfer functions for multi-layer slabs". ASHRAE Transactions, Vol. 77, pp. 117-126.
- Wang, F.S.** 1981. "Mathematical modeling and computer simulation of insulation systems in below grade applications". Proceedings of the ASHRAE Conference, Thermal Performance of the Exterior Envelopes of Buildings, New York, p. 472.

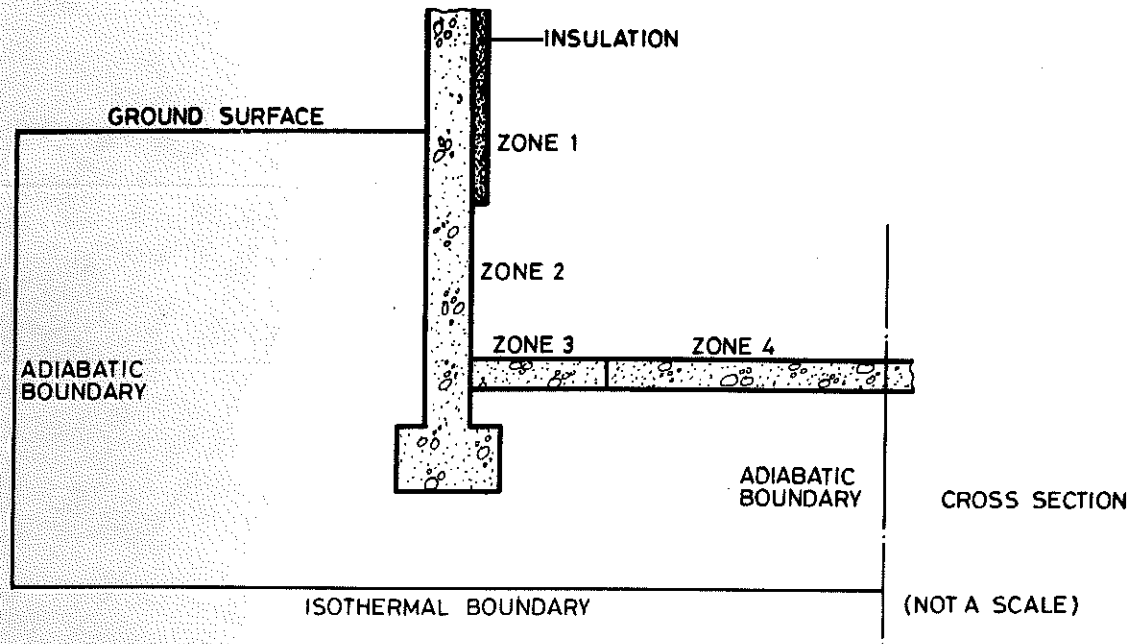


Figure 1. Cross section of the basement model (not a scale)

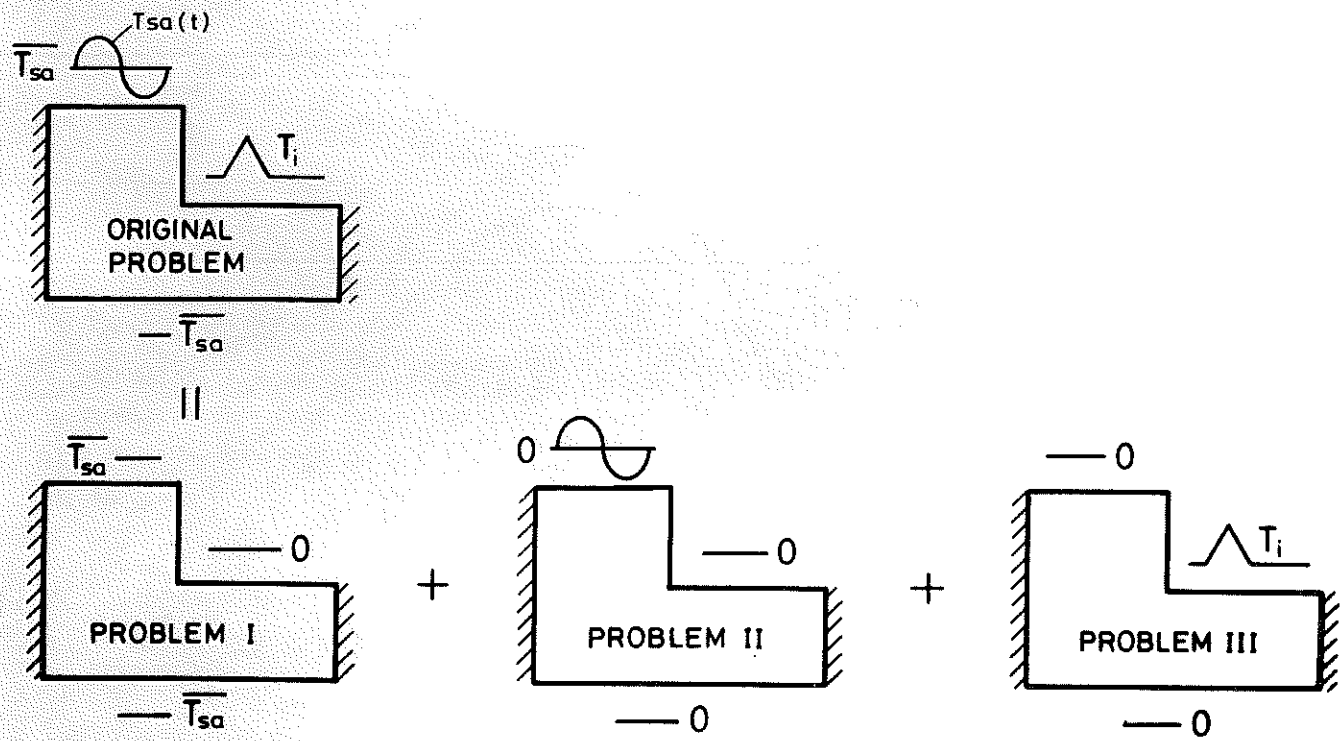


Figure 2. Application of the super-position principle

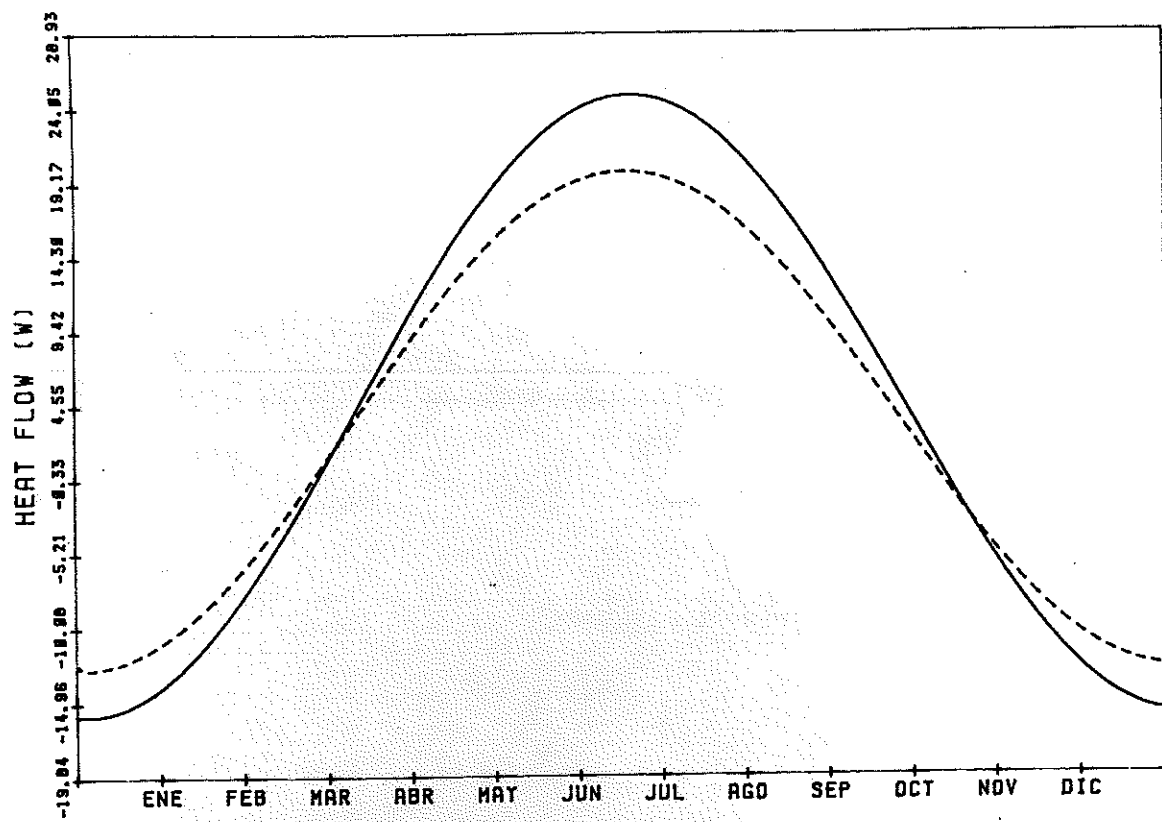


Figure 3. Heat flows in zone 1

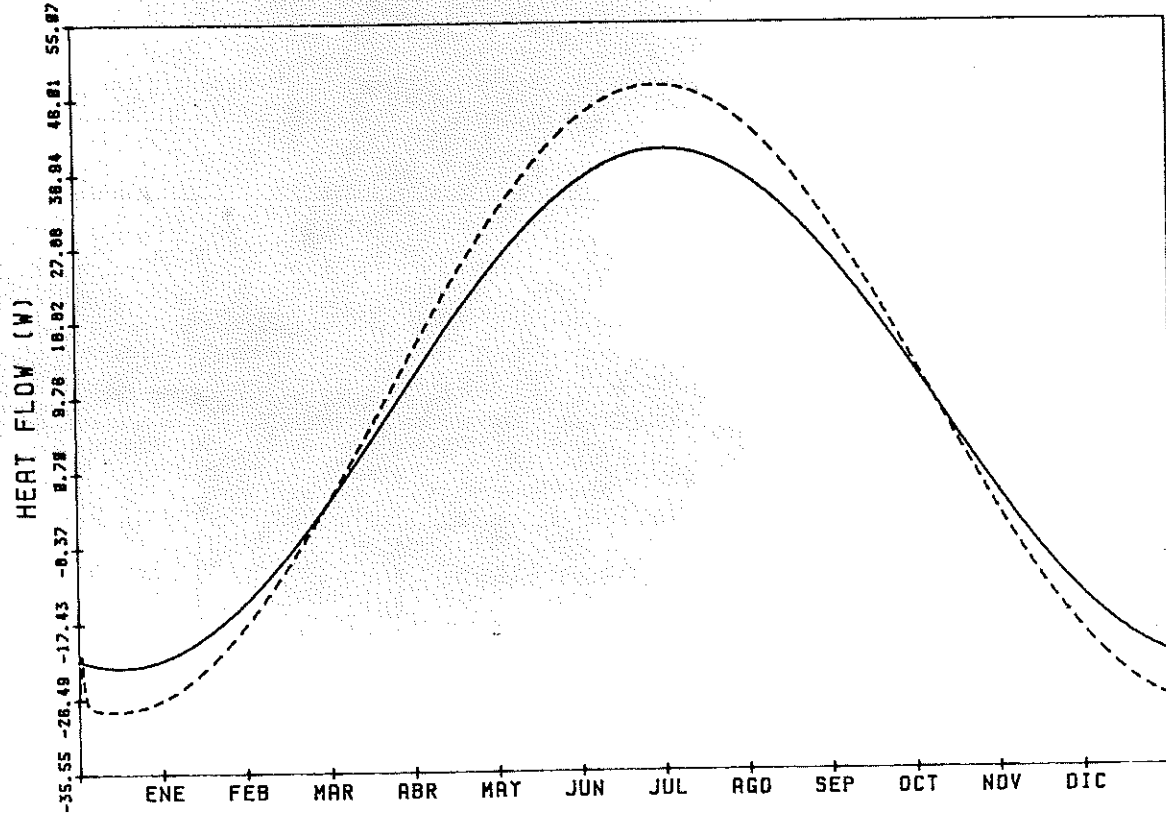


Figure 4. Heat flows in zone 2

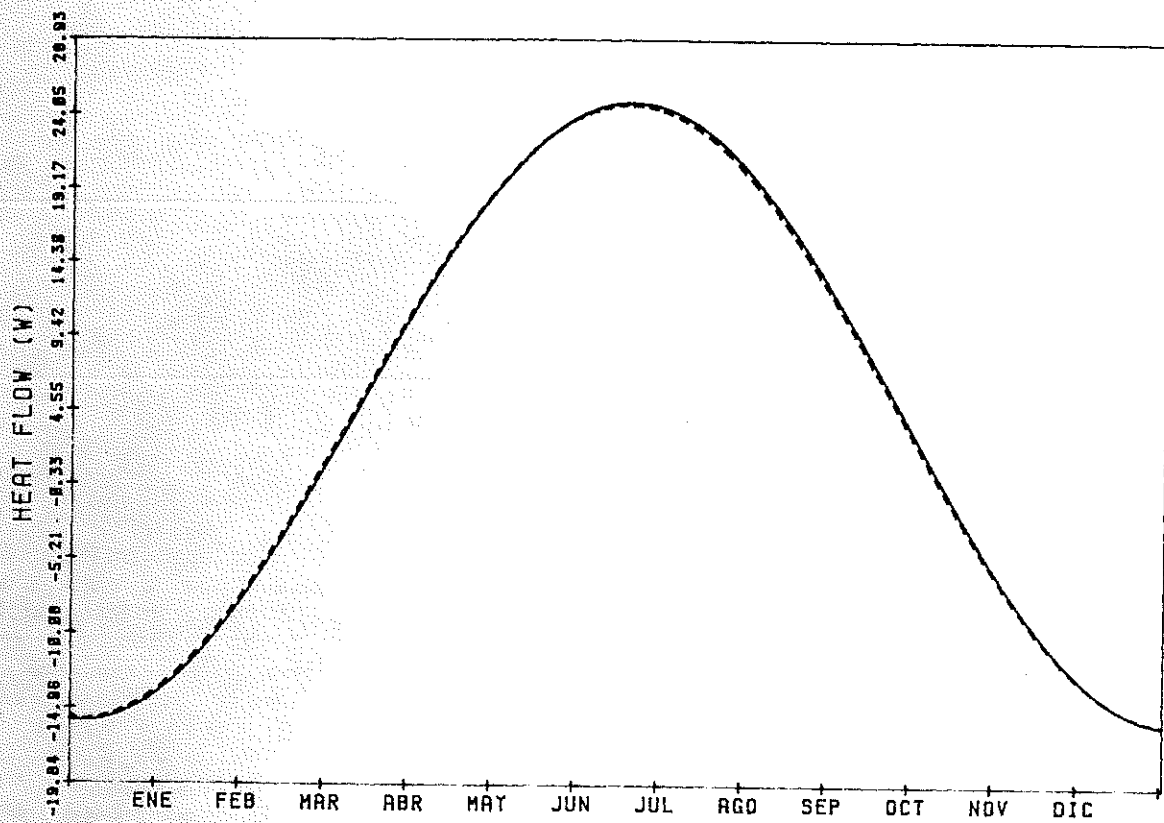


Figure 5. Heat flows in zone 1 (after correction)

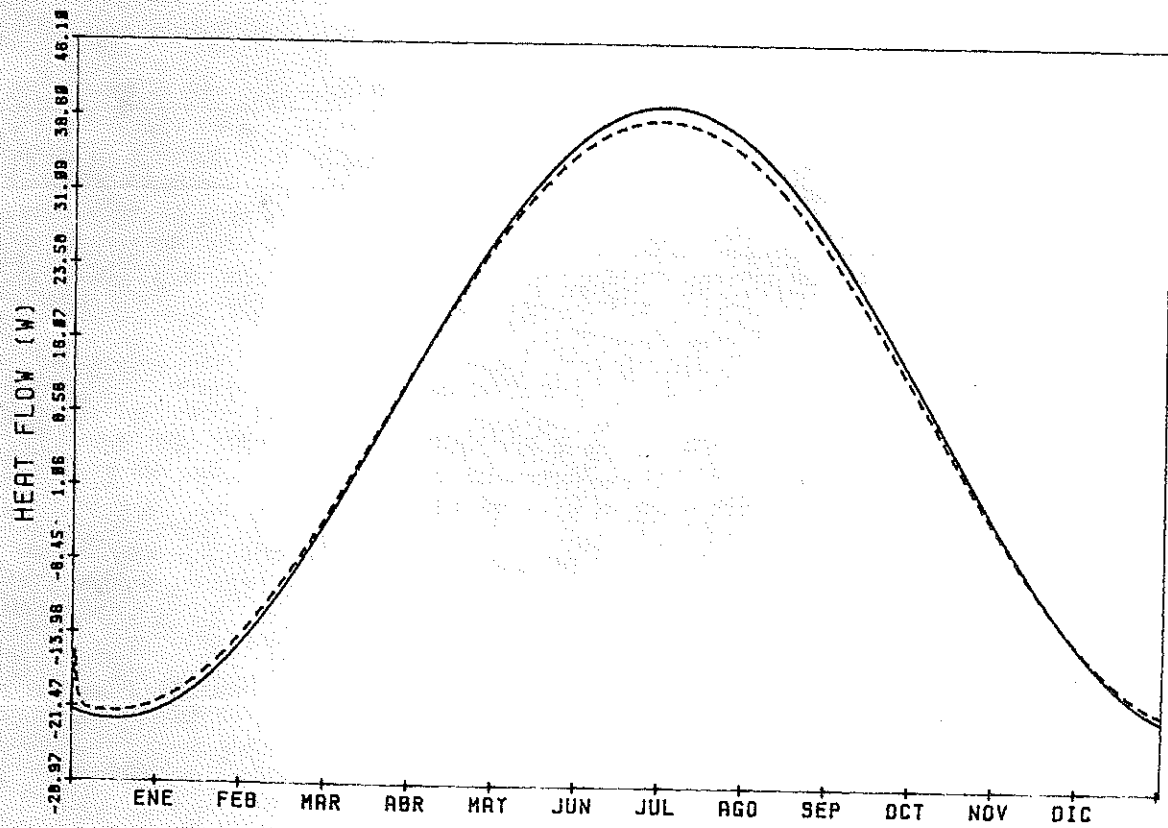


Figure 6. Heat flows in zone 2 (after correction)